International Journal of Nanoelectronics and Materials
Volume 12, No. 2, Apr 2019 [145-156]

Multi-Response Nanowire Grating-Coupled Surface Plasmon Resonance by Finite Element Method

Ali Abdulkhaleq Alwahib[1*], Wijdan H. Muttlak[1] and Ali H. Abdulhadi[1]

[1]*Laser and Optoelectronics Engineering Department, University of Technology, Baghdad, Iraq.*

Received 9 May 2018, Revised 1 October 2018, Accepted 20 October 2018

ABSTRACT

In this paper, Surface Plasmon Resonance (SPR) has been applied for sensing acetone liquid by changing the refractive index based on nanowire grating. This sensor was proposed and numerically analysed using finite element method. The SPR sensor composed of multi-nanowires distributed in a parallel order at a specific distance. These wires were deposited onto the dielectric material and tested using laser light at wavelengths between 500 nm to 700 nm. Dual SPR dips emerged at two different SPR angles after further tuning the incident angle. The multi SPR dips are angularly wide but spectrally produced very sharp results. SPR sensor results were compared at four different plasmonic materials gold, silver, aluminium and copper using 532 nm wavelength. These plasmonic materials were tested using acetone at 100%, 50%, 10% concentrations. The sensitivity measurements of the sensor have shown that the dual SPR dips can be used effectively to increase the sensitivity of the designed sensor. Both dips were also used to increase the detection sensitivity of different types of liquids. The sensitivity of SPR causes a shift in dip or intensity due to any small change in refractive index. This shift varies according to the material and liquid concentration. The sensitivity of nanowire grating was measured by varying the refractive index with the resonance angle (θ°) at a single wavelength. The highest sensitivity has been discovered for gold which is 290.57°/RIU. This work is adopted for the improvement of the surface plasmon sensor using nanowire technology. The structure is easy and simple and can be applied to different applications.

Keywords: Surface Plasmon, Sensor, SPR, Grating, Nanowire.

1. INTRODUCTION

Recent years have witnessed that the optical sensors play a distinguished role in our life due to unprecedented changes in the way sensors work [1]. Researchers intensify their effort in the design and development of new sensors that meet the current demand and applications. Different optical sensors have been designed to reduce time, cost and enhanced the daily processes [2]. However, laboratory design methods normally need significant efforts as well as different scientific fields which are mostly solved by computer simulation [3].

Simulation programs have proved to be a crucial adjunct in analysis and the identification of the sensor properties. Modelling programs solve sensor problems efficiently, safely and easily verified. Therefore, sensor modelling programs are an important aspect in most nano applications especially in during the development of selective sensors [4]. The plasmonic behaviour can be tested for different surface shapes such as circle, square, and flat surface using the simulation programs.

* Corresponding Author: *140052@uotechnology.edu.iq*

Surface Plasmon Resonance (SPR) is an electromagnetic phenomenon that occurs in a thin flat layer of conducting films deposited at the interface between two different refractive indices layers. Fibre, prism (Kretschmann and Otto configurations), grating, and waveguide configurations are convenient for generating SPRs [5][6][7]. The Kretschmann configuration consists of a plasmonic material film deposited directly onto the prism or on the glass slide attached to the prism [8][9]. When the Transverse Magnetic (TM) polarized light strikes a conducting layer such as gold at a given angle, a plasmonic wave will be generated and propagated along the interface of a thin metal layer [10]. SPRs dissipate their electromagnetic wave through metal layer interaction. The electromagnetic wave loss is due to scattering of free-electron in the plasmonic layer and, by optical absorption throughout electronic inter-band transitions [11]. This barrier has encouraged researches to understand the physics of SPR from amplification and feasibility to compensate the SPR losses.

Since the first SPR sensor which was invented in 1982 [12], different approaches have been proposed from several groups to enhance the SPR sensitivity. Each approach has wide range of variables and unique designs such as plasmonic materials, optical design (multipath), nanomaterials, supercontinuum exciting SPR, magneto-optic SPR, Fabry Perot based SPR, and Bragg grating based SPR. Furthermore, the sensitivity of SPR measurement varies significantly according to the type of dielectric (liquid or gas), and the type of configuration (prism, optical fibre and diffraction grating).

Light losses and propagation are general properties of SPR. These properties can be enhanced depending on the shape design of metal nanowires [13]. Au nanowire has attracted substantial attention in sensor applications [14] due to its ability to absorb more than 50% of low energy photons [15]. According to the literature, the benefit achieved in sensitivity throughout nanowire is ~800°/RIU [16]. The angular sensitivities sensors were reported below 100/RIU for diffraction grating-based SPR and are mostly enhanced by making the SPR dips the +1st order of the diffraction grating [17]. Extensive efforts have been devoted to achieved perfect sensitivity, including changing the plasmonic materials [18], geometrical shapes, dimensions, and the interval between the structures [19]. A comparison of acetone sensitivity based on SPR principle under different configuration is shown in Table 1.

Table 1 Comparison of acetone sensitivity under different configurations

Method	Sensitivity	Ref.
Non-invasive screening and monitoring diabetes with doped polyaniline (PANI) layer using acetone sensor	The sensor sensitive was measured from the penetration depth through the dielectric (2.68 μm). By using WinSpall SPR simulation software, the results were built based on Fresnel equations at mid-infrared wavelength (3000 nm). The shift in SPR angle for the modelling is 6.410, while it is 80 for the simulation.	[20]
Acetone Sensor based on Hierarchical 3-D TiO2 Nanoflowers is tested for Volatile Organic Compound (VOC) sensing under a low-temperature hydrothermal process	The practical results showed fast response/recovery of ~6-15s / ~15-39 s authenticated the potentiality of the sensor devices under 60ºC optimum operating condition. The response magnitude was found to be 3.45% (66.58%) with the corresponding response time of 33 s (19 s) and recovery time of 11s (37 s) for 1 ppm and 700 ppm acetone	[21]
Dual Sensing Arrays Based on Nano-wire / Nano-rod Hybrid Nanostructures for Surface Plasmon Resonance and Surface-Enhanced Raman Scattering	This configuration indicated that both Raman signals and thickness sensitivity can be enhanced by adding nanorod structures into nanowire arrays. Furthermore, it was noted that the Surface-Enhanced Raman Scattering sensitivity can be further improved when reducing the width of nanowires and the gap/width between the nanorods.	[22]

Detection of Acetone Vapor based on the reflectance on the optical and geometric properties of the sensitive over layers of the graphene film when the vapour molecules are absorbed on it.	The sensor shows accepted response upon exposure to various concentrations of acetone vapour from 44 ppm to 352 ppm. Also, it is clear that the greater the dilution of the acetone vapour, the smaller the variation in the reflected optical power	[23]

This work reports the nanowire grating using surface plasmon resonance in the liquid sensor (refractive index sensor). The experiment was conducted to use dual sensing points at different concentrations of acetone. The results also proved that SPR depends on the shape of the excited surface. Conventional mounted nanowire grating dual sensing point was proposed theoretically for a single wavelength, for the first time. In this design, the parallel notches or steps in conventional grating were replaced by the parallel nanowires.

2. THEORY

The main condition for plasmon waves generation in wire grating technique is the coupling of the tangential component of incident light with real part of plasmonic surface material [16][20]. These waves will be generated if the incident light from the side of the plasmonic material such as glass has a higher refractive index. At a specific angle, the optical absorption of incidence light will increase. When this angle equals to the SPR angle of the specific material and wavelength, the plasmonic dip reaches the maximum. The reflectivity of the plasmonic film is normal at all angles except for short range of angles around theta SPR (θ_{SPR}), where the absorption is maximum [21]. Maximum absorption will occur when the wave vector of the incident light matches the wave vector of the surface plasmons. The criterion for positive interference is that the difference in optical path length along the two paths equals the vacuum wavelengths [22]:

$$m\lambda_0 = \mathrm{d}(n_\beta sin\beta_m - n_\alpha sin\alpha) \quad (1)$$

where m = 0, ±1,± 2,..., λ_0 is the vacuum wavelength, and β_m is the transmitted diffracted beam of order m. For m = 0, the optical path reduces to refraction as described by Snell's law in Figure 1 [20]:

$$n_\beta sin\theta_\beta = n_\alpha sin\theta_\alpha \quad (2)$$

$$2\lambda_0 > dna\ (1 + \sin\alpha) \quad (3)$$

The surface plasmon (SP) wave via a diffraction grating is [23]:

$$n_d sin\theta_\alpha + m\frac{\lambda}{\Lambda} = \pm\sqrt{\frac{\varepsilon_m n_d^2}{\varepsilon_m + n_d^2}} \quad (4)$$

where θ_α is the SPR angle, '+' related to orders of diffracted waves (m > 0), and '–' related to orders of diffracted waves (m < 0). Equation (4) indicates that the resonant angle θ_α relies on the refractive index of dielectric n_d medium, thus, the diffraction configurations can be used as a refractive index sensor in angular interrogation method.

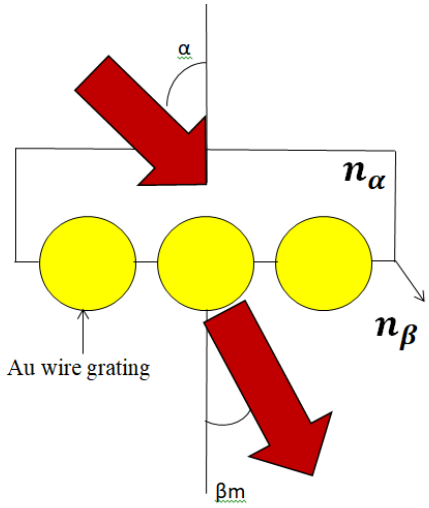

Figure 1. The optical path of Au wire grating at the plane of incidence.

The plasmonic capability of the nanowire grating depends on the polarization effects of the incident wave. For this reason, both Transverse Magnetic (TM) mode and Transverse Electric (TE) mode are applied. The electric field vector of the TE wave has additional Z direction to the existing XY- modelling plane. Whereas, the electric field component of the TM wave is perpendicular to the direction of propagation and formed the XY-plane. While the magnetic field component establishes only in the z-direction.

3. SIMULATION WORK

Finite Element Method (FEM) was adapted to enhanced nanowire grating SPR. The sensor consists of four different layers as shown in Figure 2. The layers are air, a glass of 0.3 mm thickness, Au nanowire of 80 nm diameters, and a dielectric substrate.

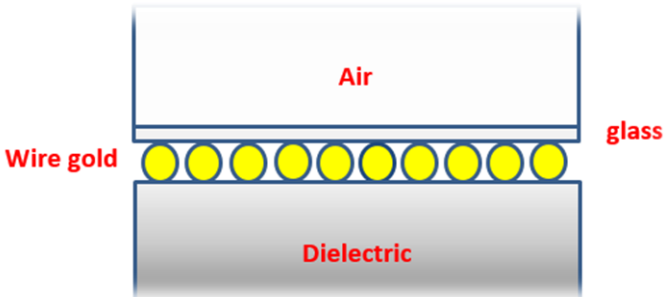

Figure 2. Nanowire grating sensor.

The model of the nanowire uses $n\alpha$ = 1 for air and $n\beta$ = 1.2 for the dielectric substrate. Furthermore, acetone and acetone are used as a dielectric substrate with different concentrations and multiple materials (Au, Ag, Al, and Cu) at circular nanowire shape.

The laser beam is projected on the first layer from the top of the designed sensor. Approximately half of the wave was absorbed by the gold wires. The presence of free electrons at the interface of two materials (gold wire with dielectric) in practice, implies that one of these materials is metal where free conduction electrons are abundant. This condition follows naturally from the analysis of a metal-dielectric interface. The angle of incidence is taken from 0 to π/2, with a pitch of π/1000. The nano-gold wire was designed with a radius of 40 nm and the

permittivity of the gold is ε = −4.6810 − 2.4266*i*. The refractive index of acetone listed in Table 2 was measured using the Lorentz-Lorenz equation provided in Equation5.

$$\frac{n_{mix}^2-1}{n_{mix}^2+2}=q1\left[\frac{n_1^2-1}{n_1^2+2}\right]+q2\left[\frac{n_2^2-1}{n_2^2+2}\right] \quad (5)$$

where n_1 and n_2 are the refractive indices of the two liquid and q1, q2 are the percentage of the liquid.

Table 2 The concentration of acetone used in the experiment

Concentration	Acetone
100%	1.359000
50%	1.343889
10%	1.332768

4. RESULTS AND DISCUSSION

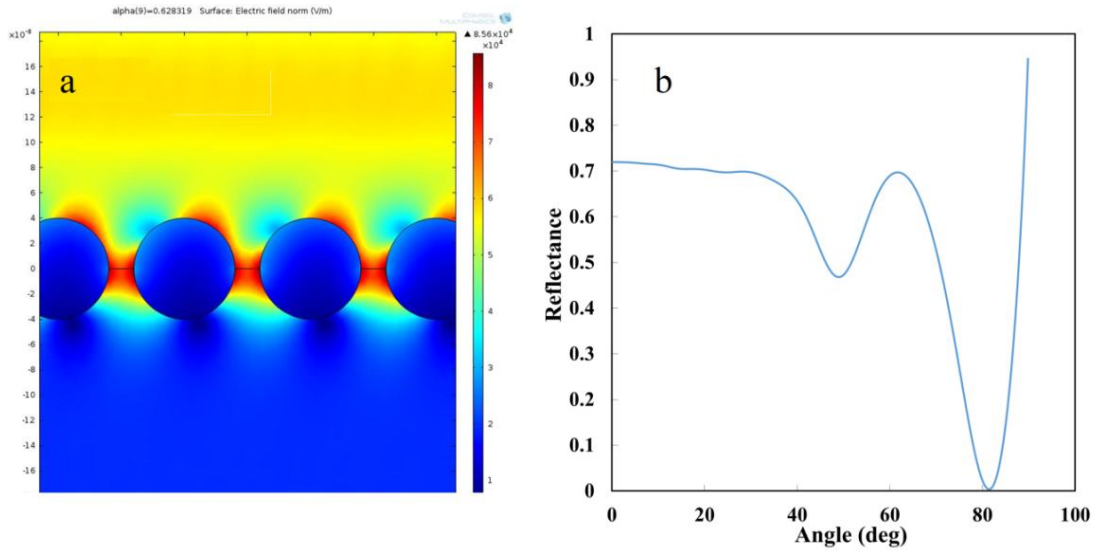

Figure 3. Nanowire grating surface plasmon circular shape.

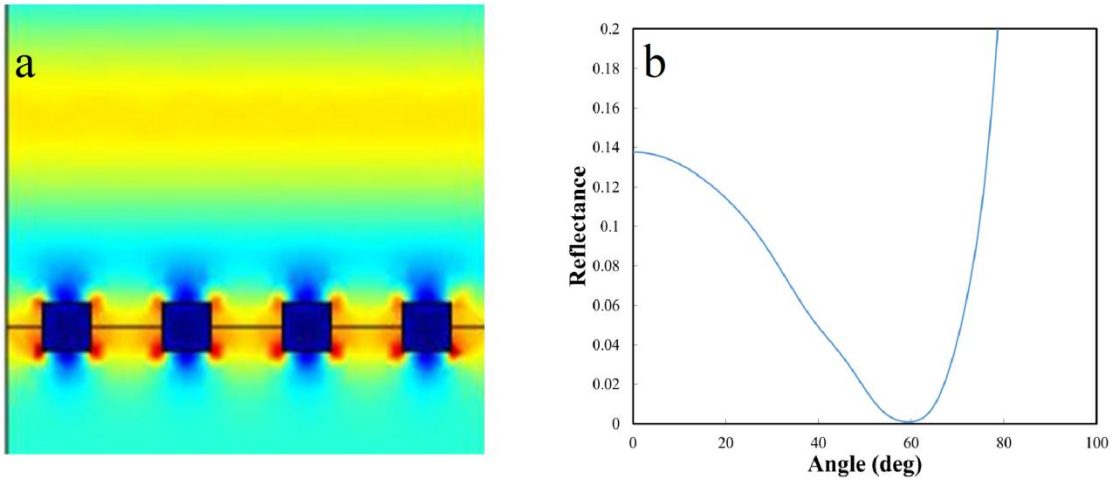

Figure 4. Nanowire grating surface plasmon square shape.

Surface plasmon response to the angle of incident and reflectance of sensing film which is a nanowire. The coupling between the incident light and the material of the nanowire depends on the wavelength of the incident light and type of plasmonic materials. Figure 3 showed the difference between the TM and TE mode using nanowire grating. The SPR excitation clearly appeared in TM mode as shown in the red and yellow regions. These colours of SPR waves generated in nanowire appeared around the top half of circle shape (where the light falls). The shape of the material surface was changed to a square shape as shown in Figure 4(a) and 4(b). The SPR curve shows a large and wide dip compared to the nanowire (circle shape) that have dual dips. The nanowire circle shape will be used and applied to the SPR sensor for detection acetone but the main key of the experiment will be the wavelengths at different plasmonic materials.

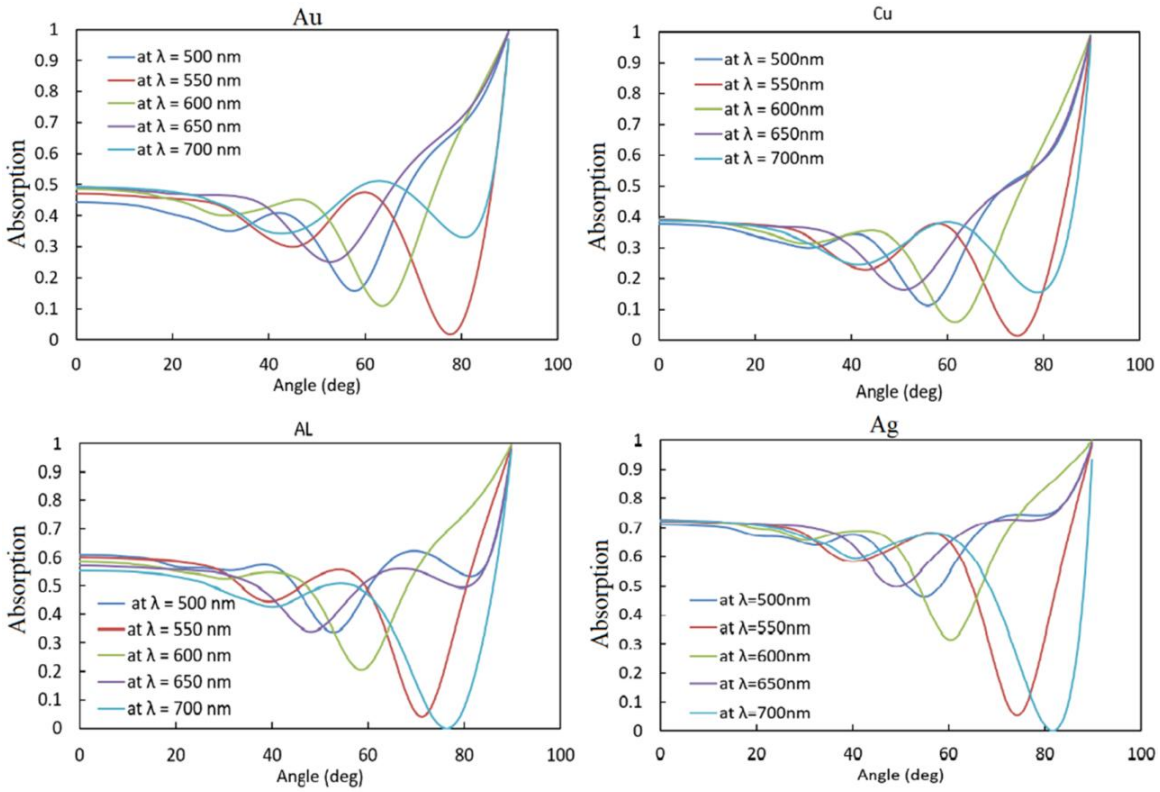

Figure 5. Absorption of different plasmonic material using nanowire grating.

The SPR has an effective relation with wavelength i.e. type of excited wavelength; short or long wavelength. In Figure 5, the reflection of the gold nanowire is varied with a wavelength between 200 to 700 nm. The result shows higher reflection for the gold nanowire at 500 nm. Plasmonic material which is the second important reference for generating surface plasmon is presented. This figure proves that using nanowire grating gives two absorption points for plasmonic materials such as gold, copper, aluminium, and silver. These absorption points have different characteristic according to the type of plasmonic material and wavelength used to excite the plasmonic waves. The best absorption points dwell between 40^{o} and 80^{o}. The best plasmonic material shown in Figure 5 is silver which has the minimum resonance dip compared to aluminium, gold, and copper.

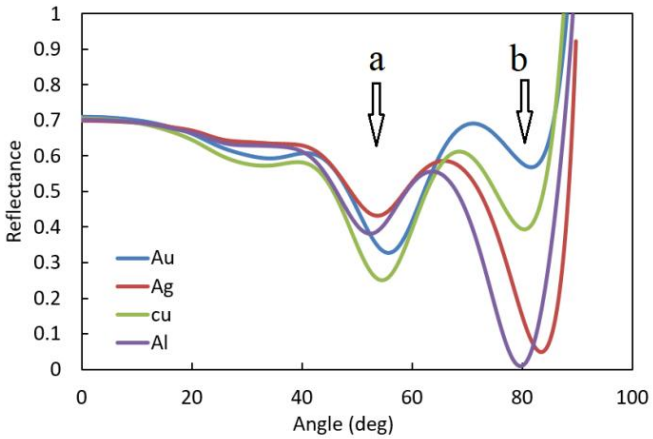

Figure 6. Plasmonic materials excited at 532 nm.

These plasmonic materials have a very strong plasmonic effect; varies according to the incident wavelength. In this research, plasmonic materials were excited using 532 nm laser wavelength as shown in Figure 6. The two-dips (a) and (b) point appeared at two different angles (different positions). The first dip (a) appeared after total internal reflection point for all test materials where the best minimum dip was copper. The second dip (b) was sharper and deeper than the first one except for gold and copper, the best minimum dip was aluminium at an angle near to 80°.

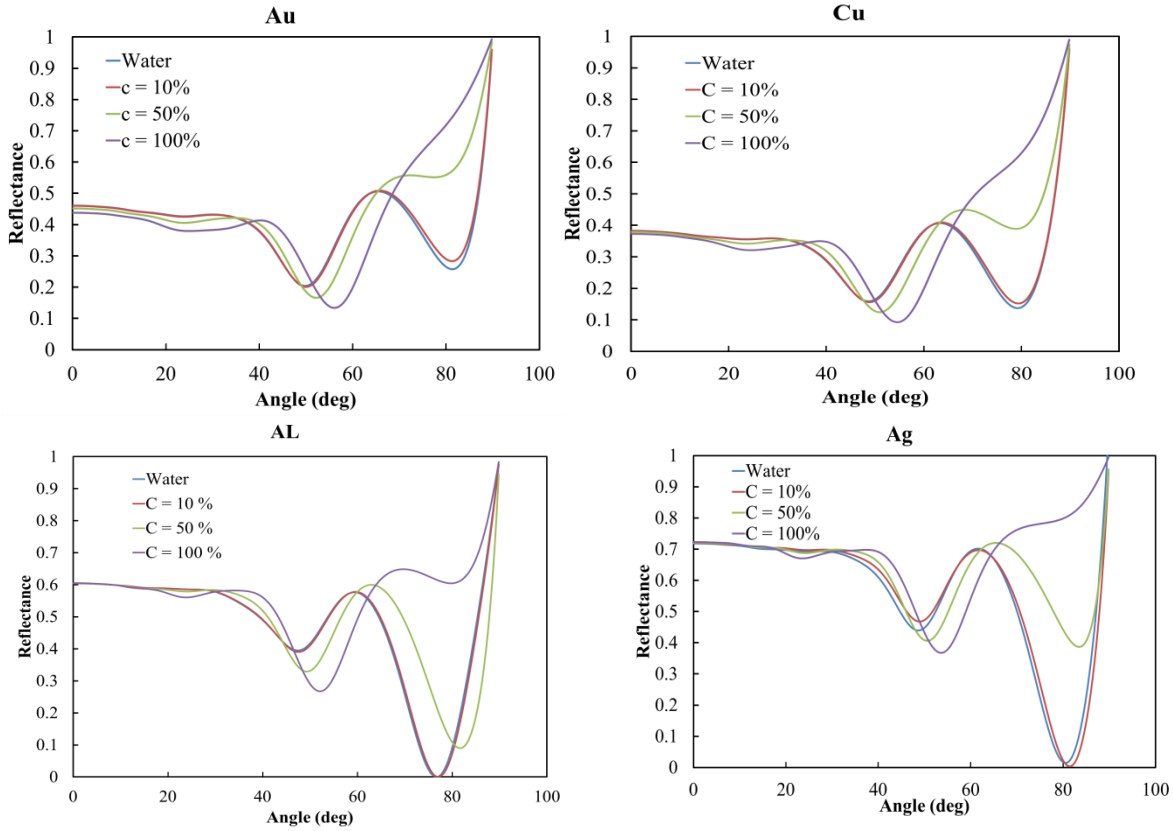

Figure 7. Acetone test at three concentrations of Au, Cu, Al, Ag.

Both dips generated from this design can be used to increase the detection sensitivity to different types of liquids, gas, and vapours. The sensitivity of SPR to a small change in refractive index will cause a shift in dip or intensity or both. In some tests, the variation of SPR dip is hard to recognize, especially if in 10^{-5} degree. So, the existing four detection points (two for angle and two for intensity) may help increase the sensitivity especially at part per billion concentrations.

Acetone was tested at different concentrations of 10%, 50% and 100% using dual dip design curve in Figure 7. The plasmonic materials Au, Cu, Al, and Ag show different shift according to the different concentrations. The first dip shifted down by increasing acetone concentrations. However, the second dip shifted up by increasing the concentrations. This shift varies according to the material and concentration. The shift can be measured by measuring the sensitivity that depends on the variation between the angle shifts. The sensitivity measurements for the tested materials were presented in Figure 8.

The sensitivity of nanowire grating-based SPR sensors variations in the refractive index can be determined by Equation (4) in θ and n_d. This results in Equation (6) [24]:

$$S = \frac{d\theta}{dn_d} = \frac{1}{n_d \cos(\theta)} \left(\pm \left(\frac{\varepsilon_{mr}}{\varepsilon_{mr} + n_d^2} \right)^{3/2} - \sin(\theta) \right) \quad (6)$$

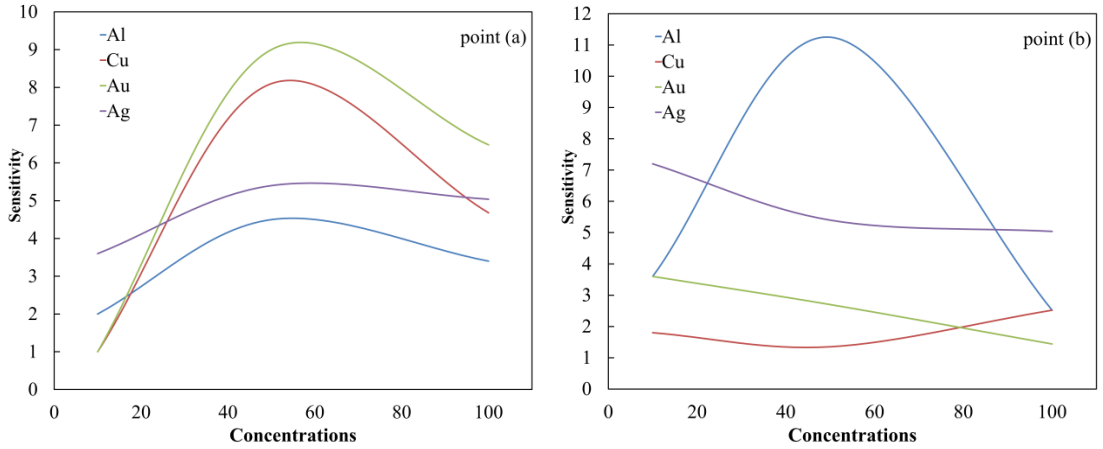

Figure 8. Sensitivity at point (a) and (b) for different plasmonic materials.

The SPR sensors coated with Ag film shows higher sensitivity compared to other plasmonic materials [25]. In Figure 8, the Au layer at point (a) shows higher sensitivity followed by Cu, Ag and Al for the first dip. The higher sensitivity gives higher stability and the sensitivity depends on the length of the sensing region and the thickness of the material. When sensitivity becomes higher, the selectivity becomes better especially at shorter wavelengths [26]. However, the measurement of sensitivity using angle interrogation is possible by multi-values. These values varied between point (a) and (b) as well as the intensity variation related to these two points. The maximum sensitivity value was at point (b) for Al layer at concentration 50%. However, the minimum sensitivity value was at point (a) for Au and Cu. The sensitivity starts and ends at a low value and maximum at the middle range of concentration.

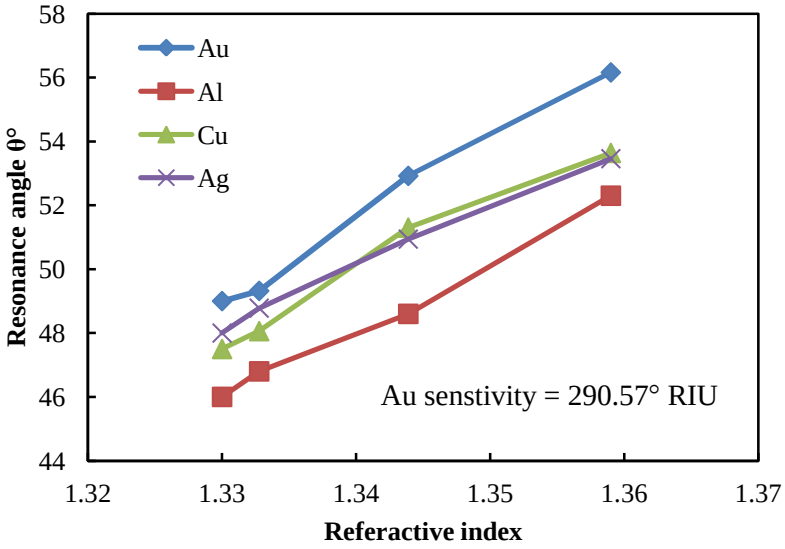

Figure 9. Analysis between SPR resonance angle and the refractive index of acetone.

SPR can be measured by coupling the resonance angle and intensity in angle interrogation method. When SPR excited at the interface between a dielectric medium and the metal surface, the optical properties such as reflectance changed drastically [27]. This change can be observed as a shift in resonance angle and the overall sensitivity is shown in Figure 9. The results of the Au, Al, Cu and Ag-based SPR diffraction grating sensors is represented as a variation of angle shift with refractive index. The sensitivities of the four cases are 290.57/RIU, 235.9/RIU, 239.95/RIU and 198.57/RIU, respectively. It is visible that in the plasmonic materials at the point (a) dip, there is a big influence on the sensitivity of the SPR sensors. From the overall materials, the Au is slightly better than the Al. However, the sensitivity at point (b) shows a lower shift in the resonance angle compared to point (a). The shift in reflectance intensity is more dependable and visible at point (b).

5. CONCLUSION

In summary, this work demonstrated that enhancement in sensitivity can be obtained in nanowire grating when multi-response points were obtained using a single wavelength. The shift in resonance angle and intensity are possible for these points. Although the lower shift in resonance angle, we can still depend on an intensity shift in SPR dip. The sensitivity for gold was 290.57/RIU, which is the better plasmonic material compared to the tested materials. The improved of the nanowire grating SPR had a linear range of sensitivity for angle shift.

REFERENCE

[1] Y. W. Fen, W. M. M. Yunus, Z. A. Talib & N. A. Yusof, "Development of surface plasmon resonance sensor for determining zinc ion using novel active nanolayers as probe," Spectrochim. Acta Part A Mol. Biomol. Spectrosc. **134** (2015) 48–52.

[2] G. Jiménez-Cadena, J. Riu & F. X. Rius, "Gas sensors based on nanostructured materials.," Analyst vol. **132**, 11 (2007) 1083–1099.

[3] D. Van Der Leer, N. P. Weatherill, R. J. Sharp & C. R. Hayes, "Modelling the diffusion of lead into drinking water," Appl. Math. Model. **26**, 6 (2002) 681–699.

[4] J. Wang, W. Lin, E. Cao, X. Xu, W. Liang & X. Zhang, "Surface plasmon resonance sensors on Raman and fluorescence spectroscopy," Sensors (Switzerland) **17,** 12, pp. 1–19, 2017.

[5] A. V. Singhal, H. Charaya & I. Lahiri, "Noble Metal Decorated Graphene-Based Gas Sensors and Their Fabrication: A Review," Crit. Rev. Solid State Mater. Sci., **42**, 6 (2017) 499–526.
[6] B. Lu, Y. Sun, X. Lai, Z. Pu, H. Yu, K. Xu, D. Li, H. D. R. I. Dqg, U. Zdyhohqjwk & V. Ri, "Side-Polished Fiber SPR Sensor With Temperature Self-compensation for Continuous Glucose Monitoring," **6**, January (2016) 411–414.
[7] B. Ran & S. G. Lipson, "Comparison between sensitivities of phase and intensity detection in surface plasmon resonance," Opt. Express **14**, 12 (2006) 5641–5650.
[8] M. Li, S. K. Cushing & N. Wu, "Plasmon-enhanced optical sensors: a review.," Analyst **140** (2015) 386–406.
[9] E. Klantsataya, P. Jia, H. Ebendorff-Heidepriem, T. M. Monro & A. François, "Plasmonic fiber optic refractometric sensors: From conventional architectures to recent design trends," Sensors (Switzerland) **17**, 1 (2017).
[10] M. Morjan, H. Züchner & K. Cammann, "Surface Science Contributions to a reliable hydrogen sensor based on surface plasmon surface resonance spectroscopy," Surf. Sci. **603**, 10–12 (2009) 1353–1359.
[11] L. Yang, J. Wang, L.-Z. Yang, Z.-D. Hu, X. Wu & G. Zheng, "Characteristics of multiple Fano resonances in waveguide-coupled surface plasmon resonance sensors based on waveguide theory," Sci. Rep. **8**, 1 (2018) 1–10.
[12] C. Nylander, B. Liedberg & T. Lind, "Gas detection by means of surface plasmon resonance," Sensors and Actuators **3**, C (1982) 79–88.
[13] M. Song, J. Dellinger, O. Demichel, M. Buret, G. Colas Des Francs, D. Zhang, E. Dujardin & A. Bouhelier, "Selective excitation of surface plasmon modes propagating in Ag nanowires," Opt. Express, **25**, 8 (2017) 9138.
[14] J. Tang, N. Qin, Y. Chong, Y. Diao, Yiliguma, Z. Wang, T. Xue, M. Jiang, J. Zhang & G. Zheng, "Nanowire arrays restore vision in blind mice," Nat. Commun. **9**, 1 (2018).
[15] N. Anttu, V. Dagytė, X. Zeng, G. Otnes & M. Borgström, "Absorption and transmission of light in III–V nanowire arrays for tandem solar cell applications," Nanotechnology **28**, 20 (2017) 205203.
[16] F. Romanato, K. H. Lee, H. K. Kang, G. Ruffato & C. C. Wong, "Sensitivity enhancement in grating coupled surface plasmon resonance by azimuthal control.," Opt. Express **17**, 14 (2009) 12145–12154.
[17] W. Su, G. Zheng & X. Li, "Design of a highly sensitive surface plasmon resonance sensor using aluminum-based diffraction grating," Opt. Commun. **285**, 21–22 (2012) 4603–4607.
[18] A. Boltasseva & H. A. Atwater, "Low-loss plasmonic metamaterials," Science (80-.). **331**, 6015 (2011) 290–291.
[19] X. Liu, Z. Huang, C. Zhu, L. Wang & J. Zang, "Out-of-Plane Designed Soft Metasurface for Tunable Surface Plasmon Polariton," Nano Lett. **18**, 2 (2018) 1435–1441.
[20] Usman, F., J. O. Dennis & F. Meriaudeau. "Development of a surface plasmon resonance acetone sensor for noninvasive screening and monitoring of diabetes." In IOP Conference Series: Materials Science and Engineering **383**, 1 (2018) 012024, IOP Publishing.
[21] Bhowmik, B., V. Manjuladevi, R. K. Gupta & P. Bhattacharyya. "Highly selective low-temperature acetone sensor based on hierarchical 3-D TiO 2 nanoflowers." IEEE Sensors Journal **16**, 10 (2016) 3488-3495.
[22] Lee, Kuang-Li, Chia-Yu Hung, Ming-Yang Pan, Tsung-Yeh Wu, Sen-Yeu Yang, & Pei-Kuen Wei. "Dual Sensing Arrays for Surface Plasmon Resonance (SPR) and Surface-Enhanced Raman Scattering (SERS) Based on Nanowire/Nanorod Hybrid Nanostructures." Advanced Materials Interfaces, (2018) 1801064.
[23] Zhang, Hang, Atul Kulkarni, Hyeongkeun Kim, Daekwang Woo, Young-Jin Kim, Byung Hee Hong, Jae-Boong Choi & Taesung Kim. "Detection of acetone vapor using graphene on polymer optical fiber." Journal of nanoscience and nanotechnology **11**, 7 (2011) 5939-5943.
[24] M. Seo, J. Lee & M. Lee, "Grating-coupled surface plasmon resonance on bulk stainless steel," Opt. Express **25**, 22 (2017) 26939.

[25] K. Kurihara & K. Suzuki, "Theoretical understanding of an absorption-based surface plasmon resonance sensor based on Kretchmann's theory," Anal. Chem., **74**, 3 (2002) 696–701.
[26] N. Mehan, V. Gupta, K. Sreenivas & A. Mansingh, "Surface plasmon resonance based refractive index sensor for liquids," Indian J. Pure Appl. Phys. **43**, November (2005) 854–858.
[27] C. Hu, "Surface plasmon resonance sensor based on diffraction grating with high sensitivity and high resolution," Opt. - Int. J. Light Electron Opt. **122**, 21 (2011) 1881–1884.
[28] I. Koudela & S. S. Yee, "Surface plasmon resonance sensors based on diffraction gratings and prism couplers: sensitivity comparison," Sensors Actuators B **54** (1999) 16–24.
[29] V. G. Kravets, R. Jalil, Y.-J. Kim, D. Ansell, D. E. Aznakayeva, B. Thackray, L. Britnell, B. D. Belle, F. Withers, I. P. Radko, Z. Han, S. I. Bozhevolnyi, K. S. Novoselov, A. K. Geim & A. N. Grigorenko, "Graphene-protected copper and silver plasmonics.," Sci. Rep. **4** (2014) 5517.
[30] P. Jahanshahi, M. Ghomeishi & F. R. M. Adikan, "Study on dielectric function models for surface plasmon resonance structure.," ScientificWorldJournal. (2014) 503749.
[31] H. R. Gwon & S. H. Lee, "A numerical approach to surface plasmon resonance sensor design with high sensitivity using single and bimetallic film structures," in plasmon resonance sensor design and bimetallic film structures, (2012).